

# Combined Effects of Geomechanical Deformation and Geometric Distribution on Flow and Transport Behaviors in Fractured Media

**Chuanyin Jiang** (Researcher)<sup>1</sup>, Xiaoguang Wang<sup>2</sup>, Chin-Fu Tsang<sup>1,3</sup>, Auli Niemi<sup>1</sup>, and Qinghua Lei<sup>1</sup>

<sup>1</sup> Department of Earth Sciences, Uppsala University, Uppsala, Sweden

<sup>2</sup> Chengdu University of Technology, Chengdu, China

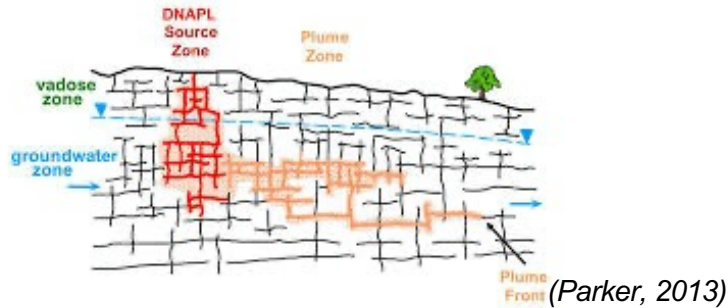
<sup>3</sup> Lawrence Berkeley National Laboratory, Berkeley, CA, USA

# Research Background

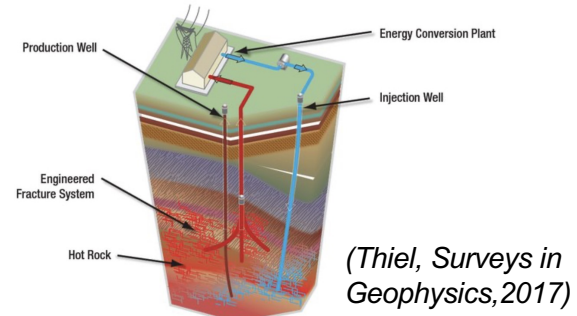


UPPSALA  
UNIVERSITET

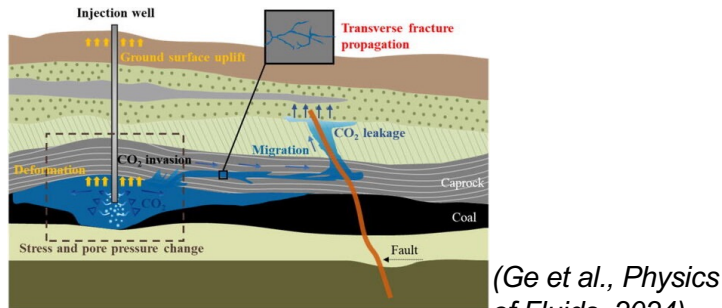
Transport in fractured media is relevant to a wide range of geoscience and geoenvironmental applications



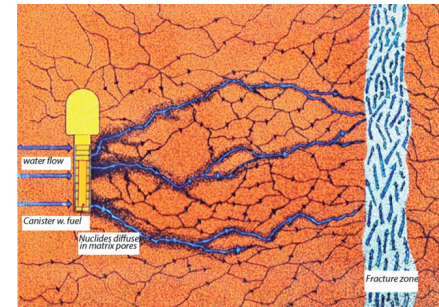
Groundwater contamination remediation



Geothermal energy development



CO<sub>2</sub> geological storage



Nuclear waste disposal

# Complexity of Transport Behavior in Fractured Media



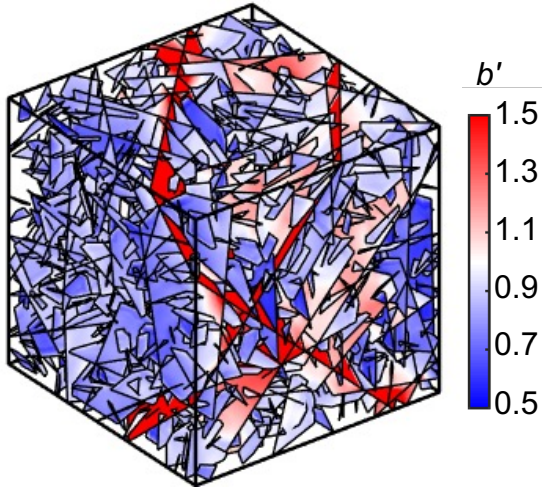
Fractured media exhibit **multi-scale heterogeneity**:

- Aperture heterogeneity at the **fracture scale**
- Topological and geometric complexity at the **network scale**

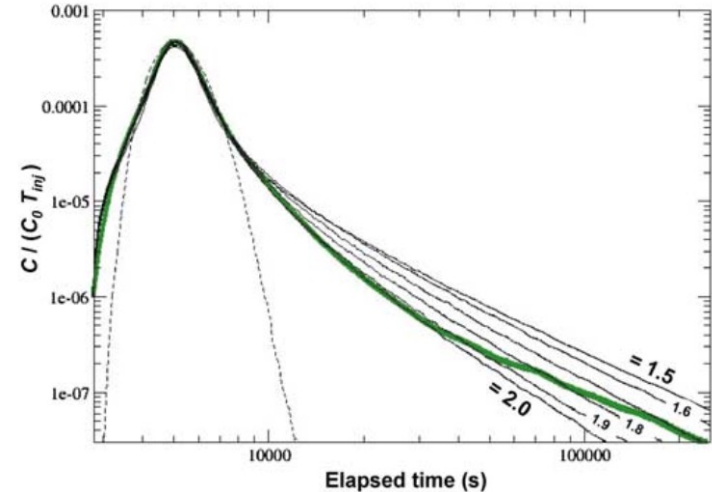


Non-Fickian transport (or anomalous transport), characterized by:

- Early arrival
- Long tailing
- Non-Gaussian solute plume



(Jiang and Lei, 2025, Computer and Geotechnics)



(Gouze et al., 2008, WRR)

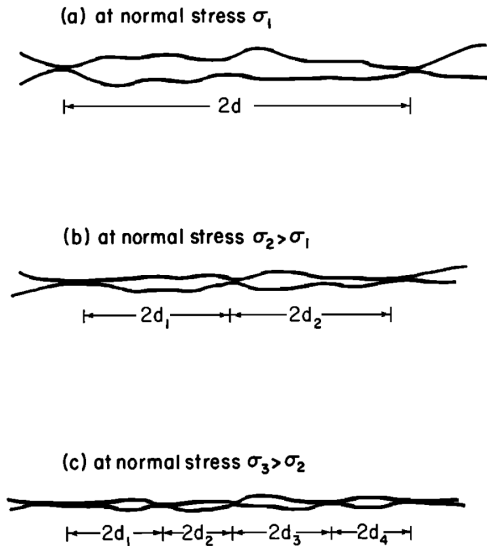
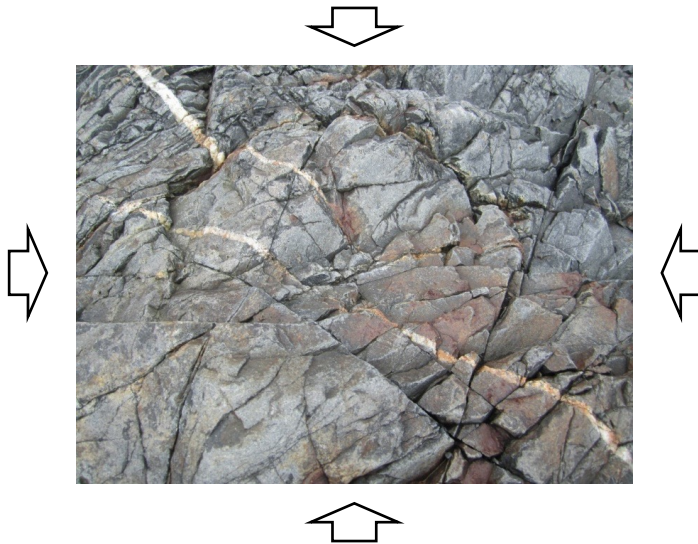
# Role of Geomechanics in Transport in Fractured Media



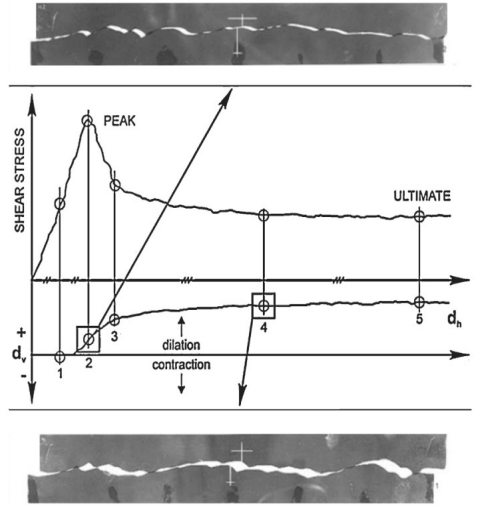
Geomechanics governs fracture aperture heterogeneity through the following mechanisms:

- Nonlinear *normal closure*,
- Shear slip-induced dilatancy (*shear dilation*),

thereby affecting the flow and transport behaviors of fractured media



Tsang and Witherspoon, 1981, JGR



Barton, 1973; Barton and Choubey, 1977

# Key Scientific Questions and Challenges



UPPSALA  
UNIVERSITET

Natural or human activities can **perturb local stress fields**, triggering abrupt changes in the heterogeneity of fracture systems. Therefore, it is important to understand how transport behaviors change accordingly, which is helpful for **upscaling**.

## Challenge of 3D DFN studies:

Geomechanical modeling requires the computation of the rock matrix deformation

→ **High computational cost** and **meshing problems** caused by the stochastic DFN geometry

Existing 3D DFN generators (e.g., dfnWorks) cannot well address the meshing problems linked with the rock matrix

## Solution:

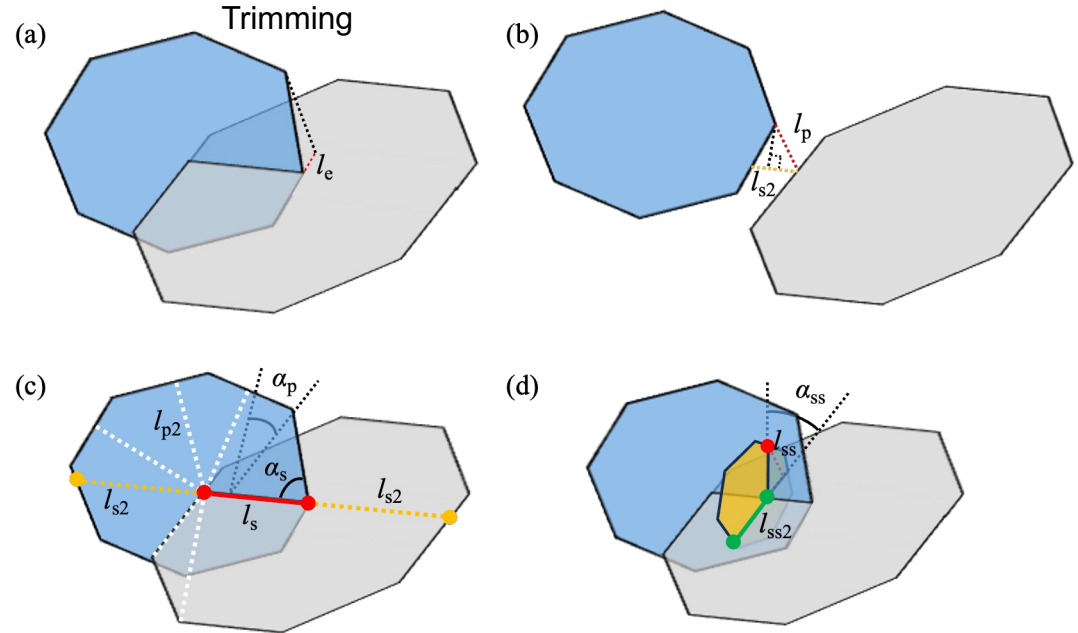
An in-house 3D DFN generator (**FracLab**) was developed, with geometric optimization functions included

# FracLab (in-house code): DFN generation with high-quality meshing



## Rejection algorithm for ensuring high mesh quality for both fracture and matrix domains

- Intersection length
- Distance between intersections
- Distance between intersection ends and polygon vertices
- 6 boundaries are regarded as 6 fractures
- Distance between intersection ends and intersection segments
- Distance between intersection ends and polygon boundaries
- Distance between polygon vertices and intersection segments
- Angle between two intersecting fractures
- Angle between the intersection segments of fractures
- Distance of polygon vertices to other polygons (to be considered in version 3)



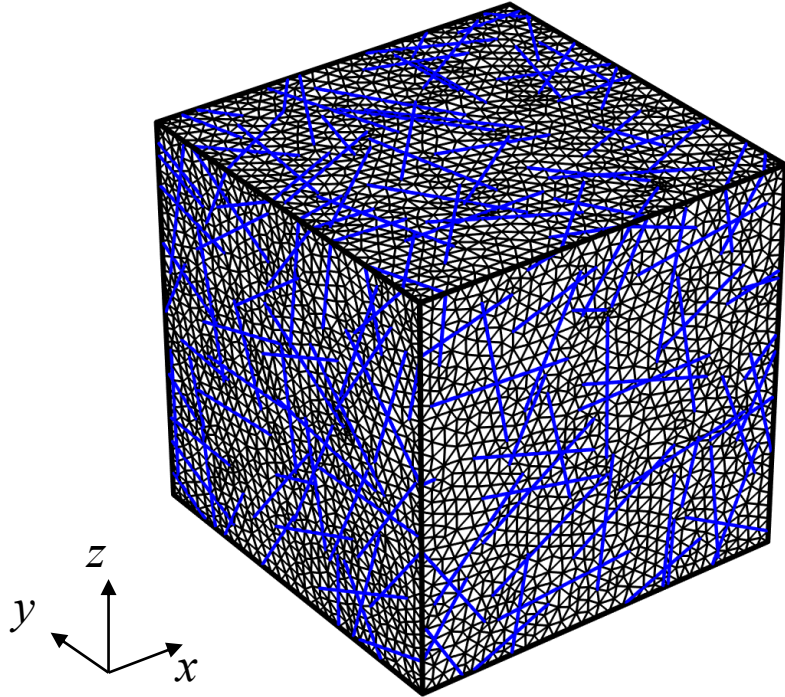
# FracLab (in-house code): DFN generation with high-quality meshing



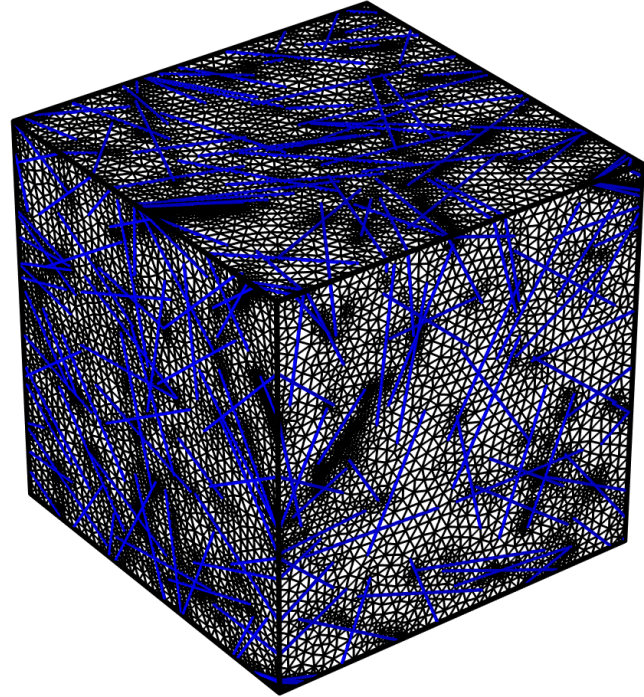
UPPSALA  
UNIVERSITET

High-quality meshing with a smaller number **enables** coupled stress-flow-transport modeling in 3D

DFN generated by **FracLab** and the meshing



DFN generated by **dfnWorks** and the meshing

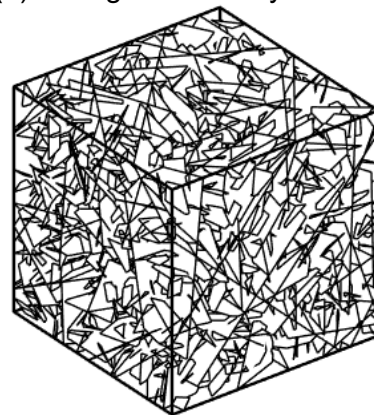


# Workflow for coupled stress-flow-transport modeling in 3D fractured media

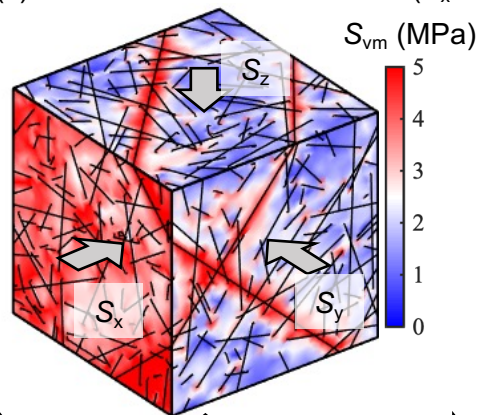
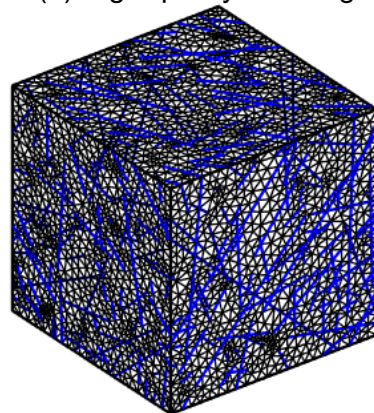


UPPSALA  
UNIVERSITET

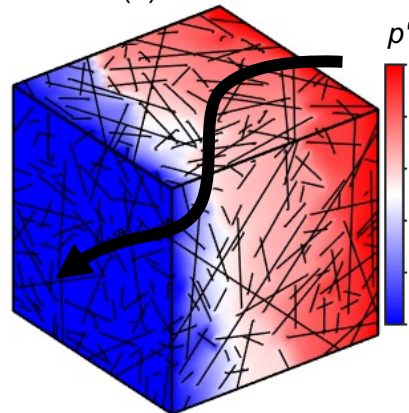
(a) DFN generation by FracLab (c) Geomechanical deformation ( $S_x = 5\text{MPa}$ ,  $S_y = S_z = 1\text{MPa}$ )



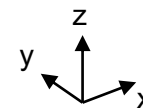
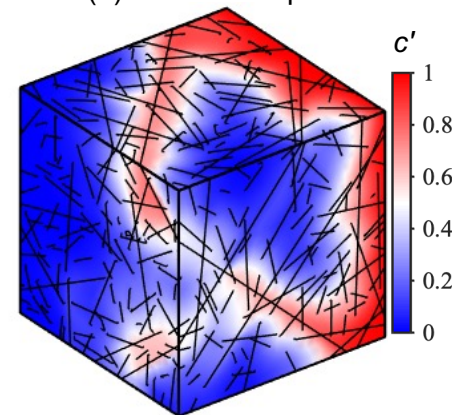
(b) High-quality meshing



(d) Fluid flow



(e) Solute transport



2 m

## One DFN example:

2000 fractures

Power-law model for radii ( $a = 3$ )

$$f(l) = \alpha r^{-a}, \quad r \in [r_{\min}, r_{\max}]$$

Orientation and positions of fractures are random

# Mathematical models



## Mechanical deformation

The quasi-static momentum balance equation for the rock matrix:

$$\nabla \cdot \boldsymbol{\sigma} + \mathbf{F} = 0$$

### Fracture-matrix interactions:

$$\boldsymbol{\sigma} \cdot \mathbf{n}_f^+ = -\alpha_f p \mathbf{I} \cdot \mathbf{n}_f^+ - \mathbf{t}_f^+$$

$$\boldsymbol{\sigma} \cdot \mathbf{n}_f^- = -\alpha_f p \mathbf{I} \cdot \mathbf{n}_f^- - \mathbf{t}_f^-$$

### Fracture mechanical behaviors:

Non-linear normal closure:

$$\sigma'_n = -\frac{K_{ni} u_n}{1 + u_n / u_m}$$

Non-linear shear slip:

$$\boldsymbol{\tau} = \min \left( \frac{\tau_c}{\|\boldsymbol{\tau}_{\text{trial}}\|}, 1 \right) \boldsymbol{\tau}_{\text{trial}}$$

$$\tau_c = \mu \sigma'_n$$

$$\boldsymbol{\tau}_{\text{trial}} = \boldsymbol{\tau}_{\text{old}} - K_s \Delta \mathbf{u}_s$$

Shear dilation:

$$\Delta u_d = \begin{cases} \tan \beta_d \Delta u_s, & 0 \leq u_s \leq u_r \\ 0, & \text{else} \end{cases}$$

## Fluid flow

$$\text{Fracture: } \nabla \cdot (\rho \mathbf{v}_m) = 0 \quad \mathbf{v}_m = -\frac{k_m}{\eta} \nabla p$$

$$\text{Rock matrix: } \nabla_{\tau} \cdot (b \rho \mathbf{v}_f) = \rho (q^+ + q^-) \quad \mathbf{v}_f = -\frac{k_f}{\eta} \nabla_{\tau} p$$

## Solute (conservative) transport

$$\text{Fracture: } \frac{\partial(\phi c)}{\partial t} + \nabla \cdot (\mathbf{v}c) = \nabla \cdot (\phi \mathbf{D} \nabla c)$$

$$\text{Rock matrix: } b \frac{\partial c}{\partial t} + \nabla_{\tau} \cdot (\mathbf{v}c) = \nabla_{\tau} \cdot (b \mathbf{D} \nabla_{\tau} c) + \zeta^+ + \zeta^-$$

Fracture mechanical aperture:

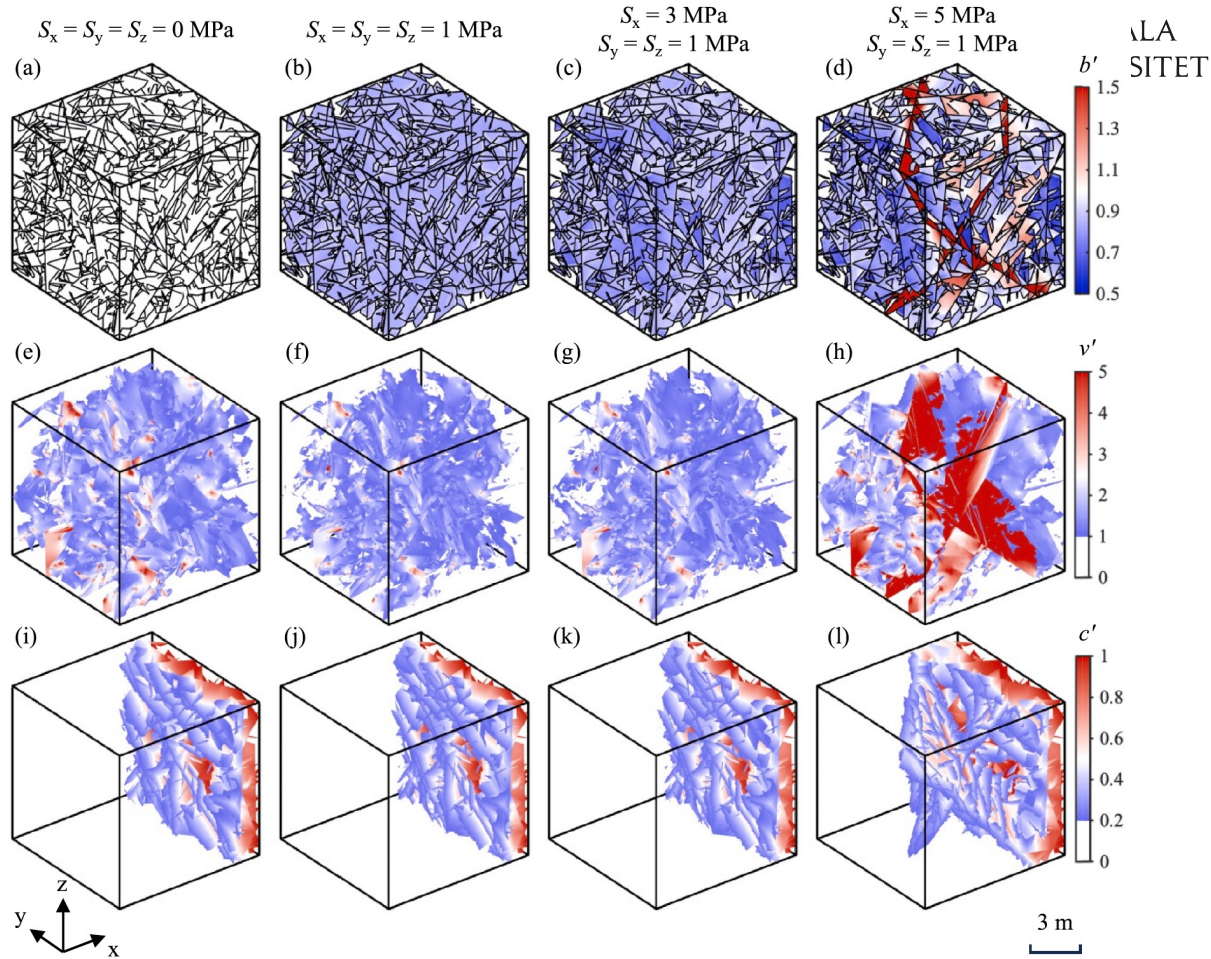
$$b = \begin{cases} b_0 + u_n, & \sigma'_n < 0 \\ b_0 + u_n + u_d, & \sigma'_n \geq 0 \end{cases}$$



# A case study with a constant initial aperture



- **Isotropic stress** -> uniform normal closure and little dilation -> no change of plume shape, and delayed breakthrough
- **Anisotropic stress with a high stress ratio** -> pronounced shearing and dilation -> strong flow channeling -> early breakthrough



# Quantitative analysis



UPPSALA

ET

Aperture heterogeneity indicator:

$$\chi = \frac{(\iint b \, dS)^2}{S \iint b^2 \, dS},$$

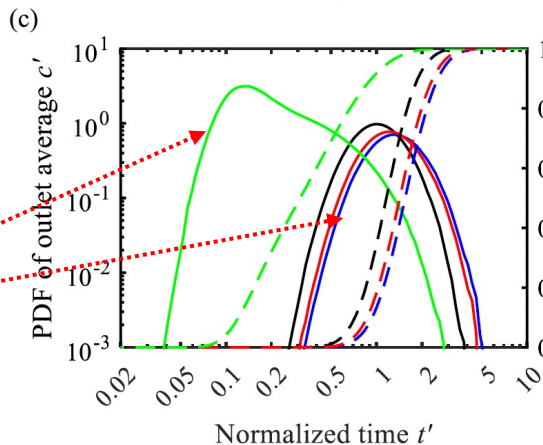
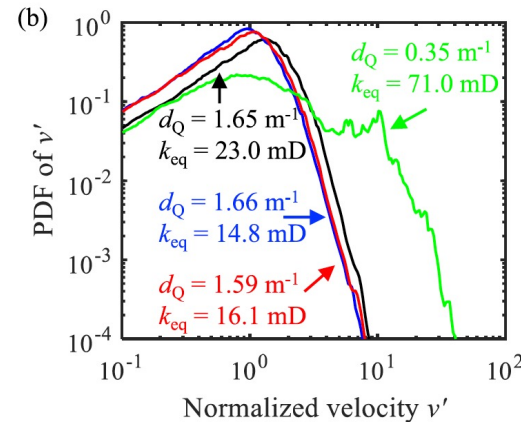
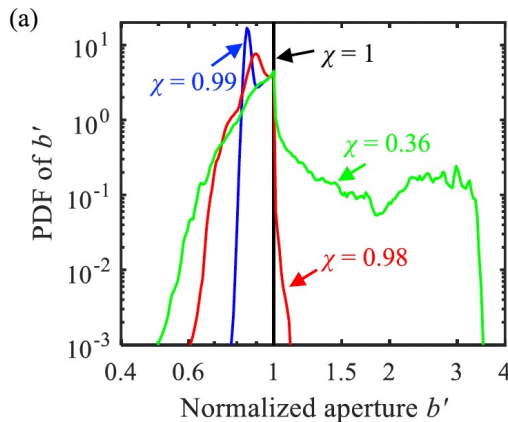
Flow channeling density indicator

$$d_Q = \frac{1}{L^3} \frac{(\iint q \, dS)^2}{\iint q^2 \, dS},$$

Equivalent permeability

$$k_{eq} = \frac{\mu Q}{L \rho g (h_{in} - h_{out})}.$$

**Stress-induced transition from Fickian to non-Fickian transport**



- $S_x = S_y = S_z = 0 \text{ MPa}$
- $S_x = S_y = S_z = 1 \text{ MPa}$
- $S_x = 3 \text{ MPa}, S_y = S_z = 1 \text{ MPa}$
- $S_x = 5 \text{ MPa}, S_y = S_z = 1 \text{ MPa}$

Solid lines: PDF

Dashed lines: CDF

# A case study with a variable initial aperture



## More realistic settings

### Aperture verifiability

Inter-fracture  $b_{0,\max} = C_1\sqrt{R}, C_1 = 5e-5$  (Olson et al., JGR, 2003)

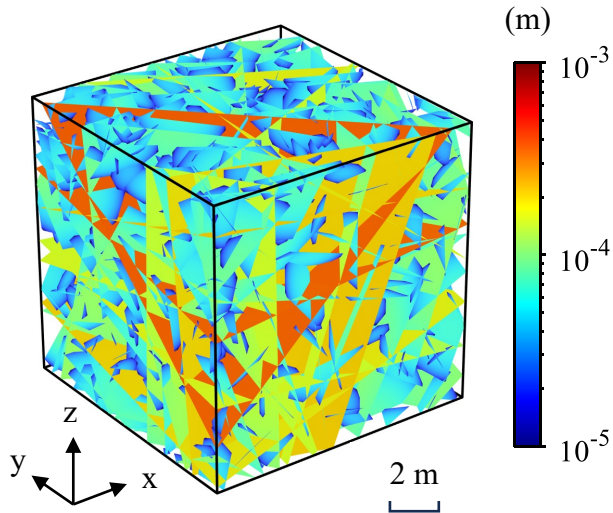
Intra-fracture  $b_0(r) = b_{0,\max}\sqrt{1 - \frac{r^2}{R^2}}$  Elliptical distribution

### Stiffness verifiability

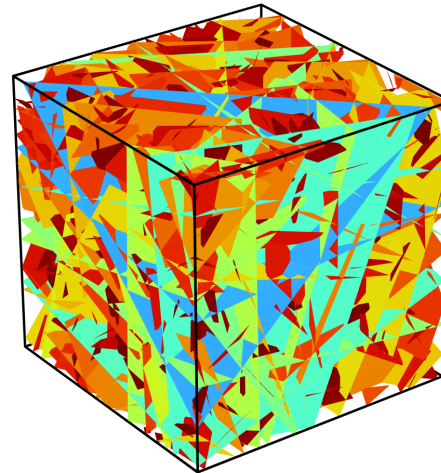
$K_{ni} = \frac{C_2}{2R}, C_2 = 600 \text{ GPa}$  (Lei, JAG, 2022)

$K_s = K_{ni} / 5$

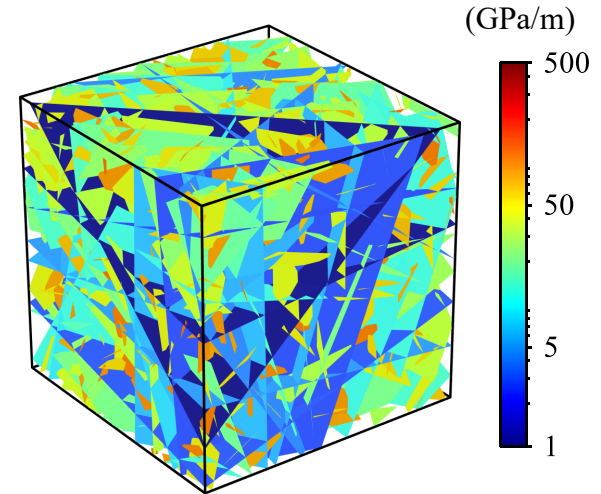
Initial aperture  $b_0$



Initial normal stiffness  $K_{ni}$



Shear stiffness  $K_s$



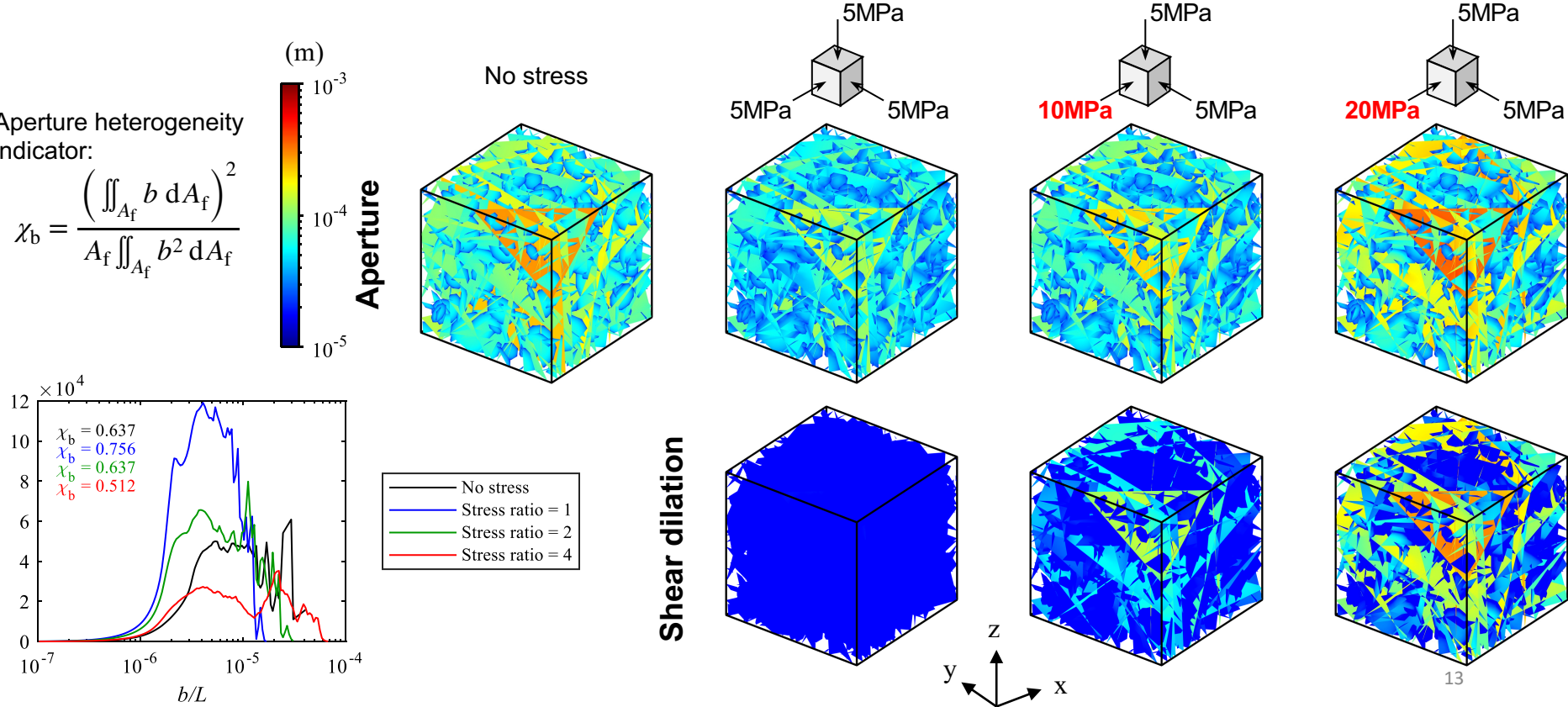
# Geomechanical deformation

Isotropic stress -> non-uniform closure -> **reduce** aperture heterogeneity

Anisotropic stress -> shear dilation -> increase aperture heterogeneity



UPPSALA  
UNIVERSITET



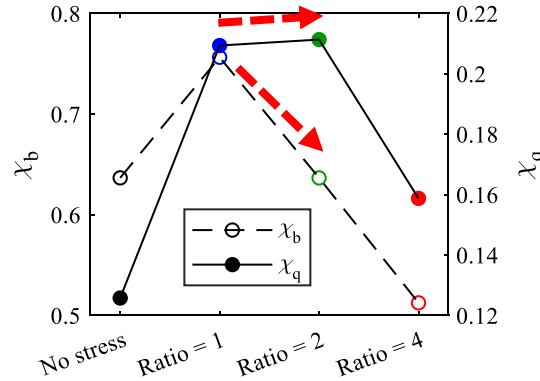
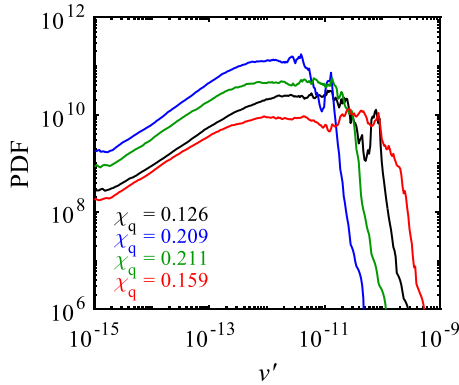
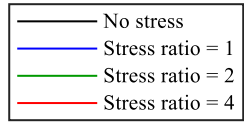
# Fluid flow

Isotropic stress -> reduce aperture heterogeneity -> weaken flow channeling

Anisotropic stress -> increase aperture heterogeneity -> **also weaken flow channeling?**



UPPSALA  
UNIVERSITET



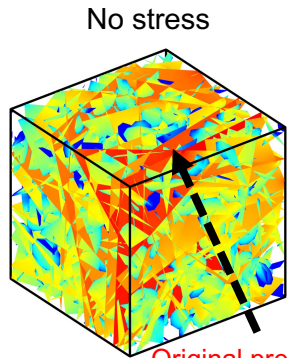
Competition exists:  
**Unstressed geometry-controlled preferential pathways** (linked with topology and size-controlled aperture)

**VS**

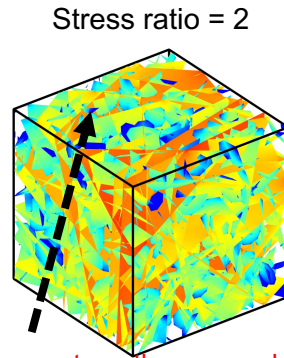
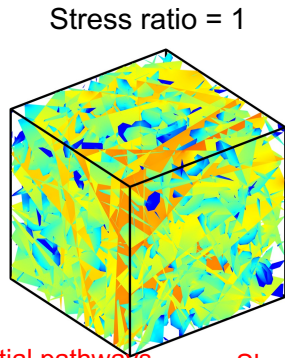
**Shear dilation-induced preferential pathways**

Flow localization indicator:

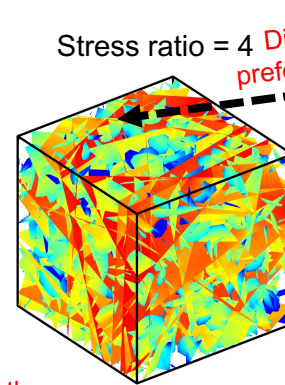
$$\chi_q = \frac{\left( \iint_{A_f} q \, dA_f \right)^2}{A_f \iint_{A_f} q^2 \, dA_f}$$



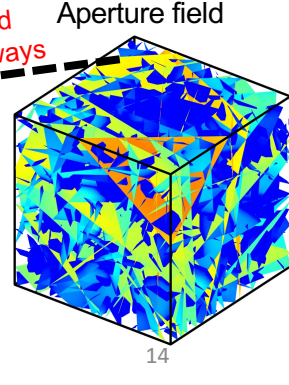
Original preferential pathways



Shearing may strengthen secondary pathways



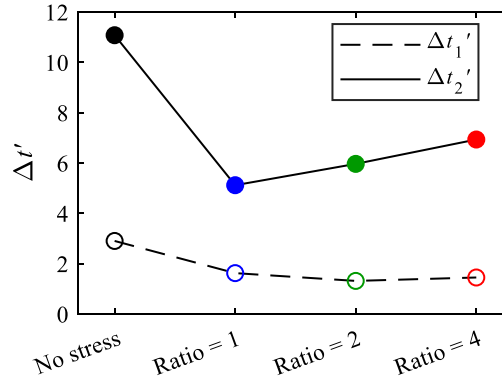
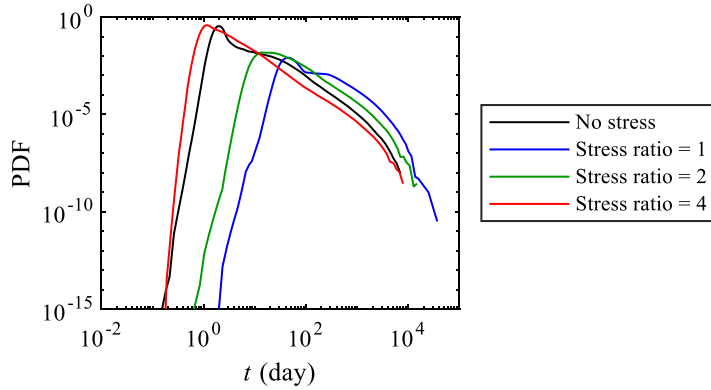
Dilation-induced preferential pathways



# Solute transport



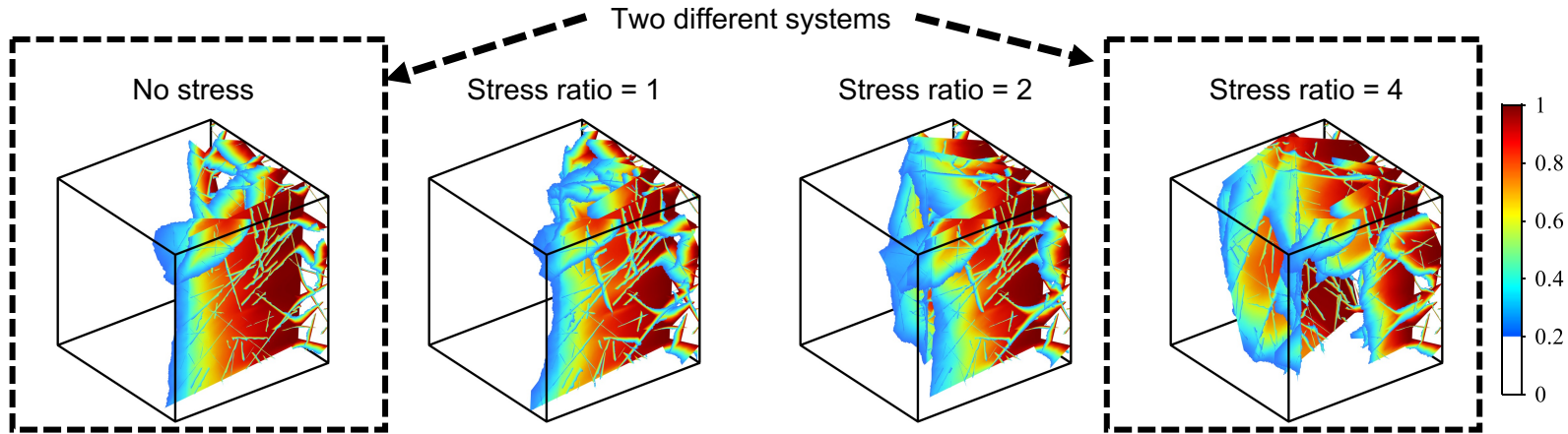
Shear dilation may **compete** with the preferential flow channels developed under unstressed conditions, promoting a more uniform flow field and even **smoothing out** the early non-Fickian breakthrough behavior.



Breakthrough time width:

$$\Delta t'_1 = \frac{t_{70} - t_{30}}{t_{50}}$$

$$\Delta t'_2 = \frac{t_{90} - t_{10}}{t_{50}} \quad \text{Impacted more by the rock matrix}$$



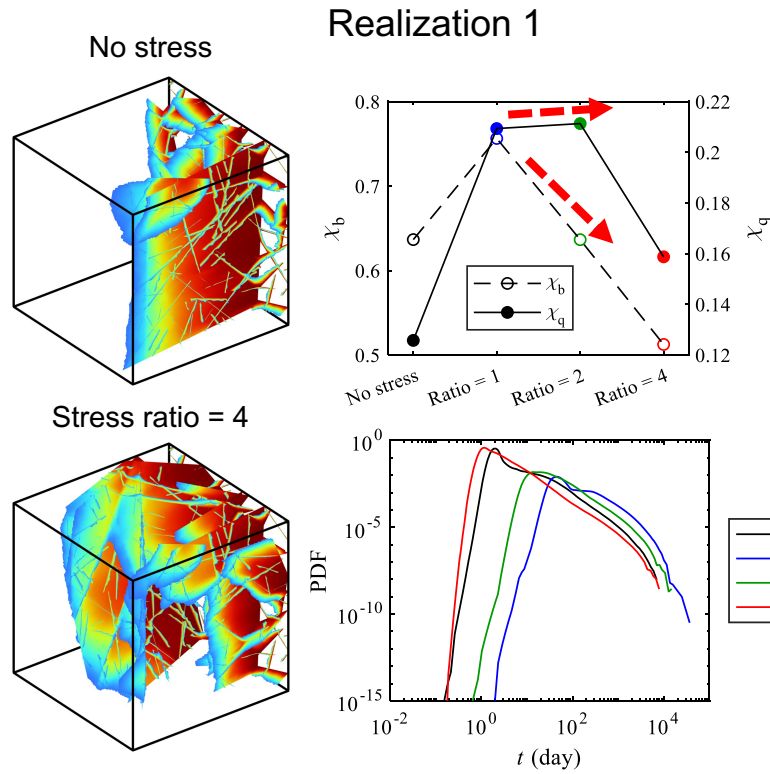
# Uncertainty of stress-dependent flow and solute transport



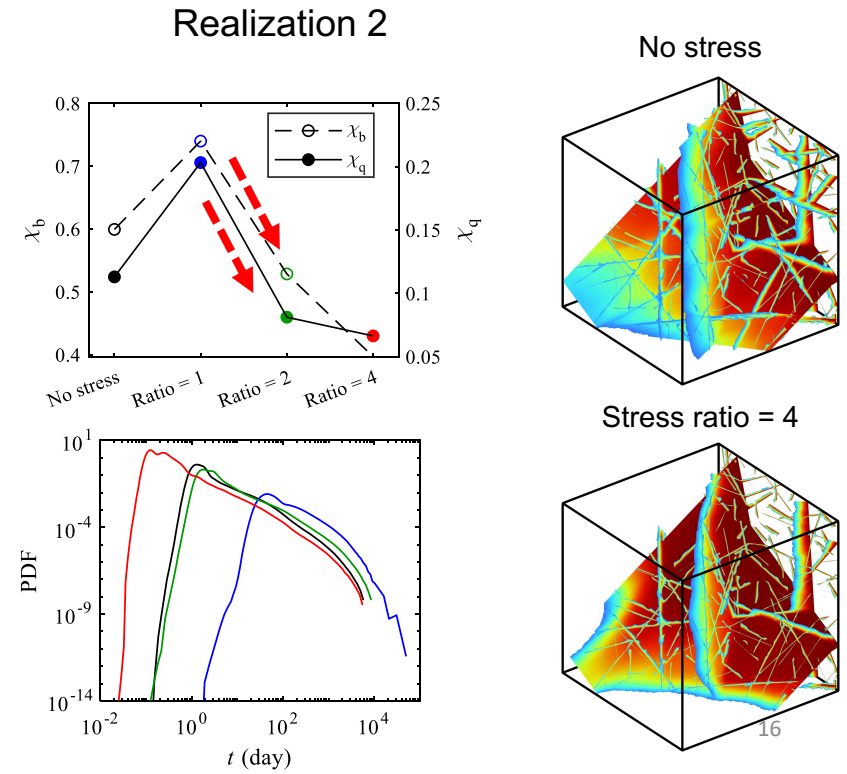
UPPSALA  
UNIVERSITET

## Geometry-controlled and dilation-induced preferential pathways

### Compete with each other



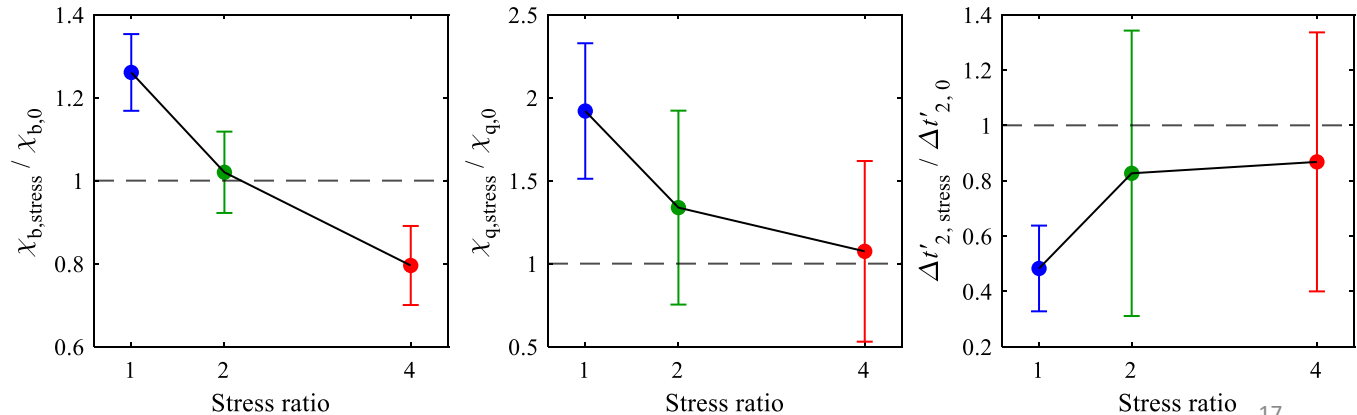
### Act synergistically



## Stress-induced non-uniqueness / stochasticity amplification:

1. Even with identical macroscopic geometric statistical parameters (e.g.,  $P_{32}$  and  $a$ ), **different realizations behave differently**: anisotropic stress loading may enhance aperture heterogeneity, but it **does not necessarily** intensify flow localization.
2. This thereby increases the uncertainty of anisotropic stress-induced flow and transport behaviors. It also significantly increases the **difficulty of upscaling**.

The ratio between the properties under stressed and unstressed conditions





Strål  
säkerhets  
myndigheten

Swedish Radiation Safety Authority



UPPSALA  
UNIVERSITET

**We gratefully acknowledge the  
Swedish Radiation Safety Authority (SSM) for  
their financial support of this project.**

**Thanks for your attention!**